applied sciences

MDPI

Article

Smart Nutrient Solution Temperature Control System for Oversummering Lettuce Cultivation Based on Adaptive Dung Beetle Optimizer-Fuzzy PID

Yuliang Cai [1,2], Zelan Zhao [2], Wenzhong Guo [2,*], Hailing Xu [3], Yunfei Teng [3], Xiaobei Han [1,2], Qian Zhao [2] and Lichun Wang [2]

[1] College of Agricultural Engineering, Jiangsu University, Zhenjiang 212013, China; caiyuliang723@163.com (Y.C.); xiaobeihan0126@gmail.com (X.H.)
[2] Intelligent Equipment Technology Research Center, Beijing Academy of Agriculture and Forestry Sciences, Beijing 100097, China; 18685053784@163.com (Z.Z.); zq1902527@163.com (Q.Z.); wlc19880323@126.com (L.W.)
[3] Beijing Jingwa Agricultural Science & Technology Innovation Center, Beijing 100201, China; hailingxu2024@163.com (H.X.); tyf202503@126.com (Y.T.)
* Correspondence: guowz@nercita.org.cn

Abstract: The summer cultivation of lettuce in greenhouses frequently encounters heat stress challenges. In hydroponic systems, cooling the nutrient solution to reduce root zone temperature is an effective strategy to alleviate heat stress. To address the issue of temperature control instability in hydroponic nutrient solutions under high-temperature conditions, this study developed a nutrient solution temperature control system based on an adaptive DBO-fuzzy PID controller. Firstly, the system integrates high-precision sensor networks and air-source heat pump units, forming the hardware foundation. Simultaneously, a fuzzy PID controller optimized by the Dung Beetle Optimizer (DBO) algorithm was designed for this system, enabling real-time adjustment of quantization and scaling factors in the fuzzy controller. Simulation results showed that the DBO-Fuzzy PID achieved a settling time of 35.23 s, overshoot of 2.18%, and steady-state error of 0.009 °C. The DBO-Fuzzy PID controller exhibited faster and more stable disturbance rejection compared to traditional PID and fuzzy PID control, demonstrating enhanced stability and robustness. System performance tests in the summer greenhouse demonstrated that with a setpoint of 22 °C, the DBO-Fuzzy PID optimized nutrient solution temperature control system maintained an average temperature of 21.98 °C, closer to the target value and exhibiting better adaptability to high-temperature environments compared to traditional PID control. Cultivation experiments confirmed the system's effectiveness in mitigating heat stress and maintaining optimal nutrient solution temperature for lettuce growth. The results can provide a theoretical basis and practical reference for precise and stable temperature control in hydroponic nutrient solutions.

Keywords: nutrient solution; root zone; temperature control; lettuce; fuzzy PID; dung beetle optimizer

check for updates

Academic Editor: José Miguel Molina Martínez

Received: 23 March 2025
Revised: 22 April 2025
Accepted: 29 April 2025
Published: 12 May 2025

Citation: Cai, Y.; Zhao, Z.; Guo, W.; Xu, H.; Teng, Y.; Han, X.; Zhao, Q.; Wang, L. Smart Nutrient Solution Temperature Control System for Oversummering Lettuce Cultivation Based on Adaptive Dung Beetle Optimizer-Fuzzy PID. *Appl. Sci.* **2025**, *15*, 5381. https://doi.org/10.3390/app15105381

Copyright: © 2025 by the authors. Licensee MDPI, Basel, Switzerland. This article is an open access article distributed under the terms and conditions of the Creative Commons Attribution (CC BY) license (https://creativecommons.org/licenses/by/4.0/).

1. Introduction

With the intensification of global warming, summer heat stress has emerged as a critical limiting factor in greenhouse vegetable cultivation [1]. Lettuce (*Lactuca sativa* L.), a widely cultivated semi-cold-resistant vegetable, thrives in cool and humid climates and exhibits poor heat tolerance [2]. Its summer cultivation frequently encounters heat stress challenges [3,4], necessitating production in specific cool-climate regions or facilities

equipped with cooling capabilities. Excessive growth temperatures can lead to developmental abnormalities, yield reduction, and premature bolting in lettuce. To ensure successful summer cultivation of lettuce in high-temperature environments, traditional cooling methods typically focus on air temperature regulation within greenhouses [5]. However, during summer, indoor temperatures in greenhouses are often extreme and susceptible to fluctuations influenced by solar radiation [6], resulting in significant temperature variability, high energy consumption for regulation [7], and limited effectiveness in controlling the root-zone microenvironment. In contrast, localized cooling strategies, particularly root-zone temperature control, have demonstrated superior energy efficiency, rapid response, and effectiveness for summer lettuce production [8], emerging as a viable alternative that has attracted extensive research attention. Studies have demonstrated that root-zone cooling can significantly enhance lettuce yield and quality [9,10], potentially enabling commercial-scale summer production [11]. This approach not only mitigates direct damage from elevated root-zone temperatures but also alleviates heat stress effects on aboveground plant parts. Consequently, developing advanced and intelligent root-zone cooling technologies represents a crucial pathway for achieving high-quality and high-yield summer lettuce production.

Soilless cultivation techniques, including hydroponics and substrate culture, have enhanced the feasibility of regulating root-zone environments by replacing soil with nutrient solutions or growth media [12,13], offering innovative approaches to mitigate heat stress. In hydroponic systems, the majority of plant roots grow directly within the nutrient solution, absorbing essential water and nutrients [14]. The temperature of the nutrient solution directly influences root-zone temperature, enabling precise regulation through heating or cooling. Although nutrient solutions exhibit greater thermal buffering capacity compared to air, they still rapidly absorb heat under intense light and high-temperature conditions, often exceeding 30 °C [15]. Elevated temperatures reduce dissolved oxygen concentration in the nutrient solution [16], accelerate root respiration, promote root senescence, and inhibit water and nutrient uptake [17]. Myung et al. developed a root-zone temperature control system utilizing an air-source heat pump [18], which achieved enhanced pepper growth and yield through nutrient solution cooling and chilled water circulation. While this system effectively reduced average root-zone temperatures during cultivation, it faced challenges in maintaining nutrient solution temperature stability during peak daytime heat, with deviations up to 6 °C from set values. Furthermore, research indicates that plants exhibit greater sensitivity to root-zone temperature variations than air temperature fluctuations, with even 1 °C changes potentially causing significant growth alterations [19,20]. Given the rapid advancement of hydroponic technologies, developing more precise and stable nutrient solution temperature control systems in high-temperature environments may represent a promising research direction.

In the field of temperature control, Proportional–Integral–Derivative (PID) controllers have been extensively utilized due to their structural simplicity and implementation convenience [21]. Taler et al. designed a digital PID controller to maintain constant hot water temperature in storage tanks [22], demonstrating significant improvements in control speed and accuracy through the reduction in random errors in temperature measurement. However, the tuning of PID controller parameters is critical to its performance. Conventional empirical or formula-based methods are often time-consuming and lack sufficient precision, particularly in adapting to complex environmental variations. Recent advancements in intelligent PID control have opened new research directions for parameter optimization. He et al. integrated fuzzy control with PID algorithms (fuzzy PID) to develop a temperature control system for calf milk replacer solutions [23]. This hybrid approach effectively addressed system uncertainties and nonlinearities by combining the adaptive parameter

tuning capability of fuzzy logic with the precision of PID algorithms. Sheng et al. implemented a fuzzy PID-based temperature controller in a multi-channel circulating biomass hot air furnace [24], achieving enhanced efficiency and quality in drying processes through fuzzy logic-driven adaptive PID parameter adjustment. However, the critical parameters of fuzzy controllers are typically determined through engineering experience and remain static post-calibration, leaving room for further optimization. Teng et al. applied Particle Swarm Optimization (PSO) to fuzzy PID controllers (PSO-Fuzzy PID) in litchi steam preservation equipment [25], demonstrating superior performance in disturbance adjustment time and overshoot control compared to conventional methods. Nevertheless, the inherent tendency of PSO towards local optima compromises global optimization accuracy. Meng et al. optimized fuzzy PID temperature control in vacuum annealing furnaces using Genetic Algorithms (GA-Fuzzy PID) [26], achieving notable improvements in control precision, response time, and overshoot reduction, albeit with compromised real-time performance due to GA's computational complexity. Qing et al. proposed a Whale Optimization Algorithm (WOA)-enhanced fuzzy PID controller for compressor speed regulation in cabin temperature control systems [27], which exhibited exceptional control performance but faced challenges in convergence speed and sensitivity to initial parameter configurations.

The Dung Beetle Optimizer (DBO), proposed by Shen et al. in 2022 [28], represents a bio-inspired optimization algorithm based on the social behaviors of dung beetle populations. Distinct from conventional optimization algorithms, DBO demonstrates superior convergence speed, precision, and stability [29]. Rehman et al. devised an integrated renewable energy system for power generation and green hydrogen production [30], employing DBO to determine the optimal capacity configuration. The optimized system achieved a reduced levelized cost of energy, establishing its competitiveness for large-scale hydrogen production. Long et al. developed an automatic throttle control system to regulate wellhead backpressure during drilling operations [31], where DBO was utilized to fine-tune PID controller parameters, thereby enhancing safety in oil and gas resource extraction. Zhong et al. integrated DBO with support vector machines (DBO-SVR) for soil nutrient prediction [32], demonstrating its adaptability to machine learning applications. Based on the above research, DBO has demonstrated significant potential across cost optimization, industrial control, and machine learning domains. However, its application to nutrient solution temperature control optimization remains underexplored, warranting further investigation to address this research gap.

This study developed a nutrient solution temperature control system based on an adaptive DBO-fuzzy PID controller for summer hydroponic lettuce cultivation. The article aims to address the issue of temperature control instability in hydroponic nutrient solutions under high-temperature conditions while bridging the application gap of intelligent control algorithms in this domain. Firstly, the system integrates high-precision sensor networks and air-source heat pump units, forming the hardware foundation of the system. Simultaneously, a fuzzy PID controller optimized by the DBO algorithm was designed for this system, enabling real-time adjustment of quantization and scaling factors in the fuzzy controller. Then, to evaluate the system's temperature control accuracy and performance metrics, simulation comparison tests, temperature control tests, and cultivation tests were conducted. These investigations assessed the system's accuracy, stability, and practical applicability, providing a theoretical foundation and practical reference for precise and stable temperature control in hydroponic nutrient solutions.

2. Materials and Methods

2.1. Test Area

In this study, the experiment was conducted in August 2024 within a plastic greenhouse located at the Jingwa Technology Demonstration Park in Pinggu District, Beijing (40°18′ N, 116°95′ E). The study area is shown in Figure 1. Situated in northern China, the region experiences a warm temperate, semi-humid, and semi-arid monsoon climate characterized by high temperatures and abundant rainfall during the summer. Consequently, the elevated temperatures inside the greenhouse posed significant constraints on lettuce cultivation. The greenhouse, spanning 24 m × 90 m (2160 m^2), was equipped with a Nutrient Film Technique (NFT) hydroponic cultivation system, which included automated nutrient solution preparation and circulation devices. During the experiment, a shielded data logger (FK-TH706) was employed to measure indoor air temperature and humidity, with the sensors positioned at the same height as the cultivation beds. The daily variations in air temperature and humidity inside the greenhouse in August are illustrated in Figure 2.

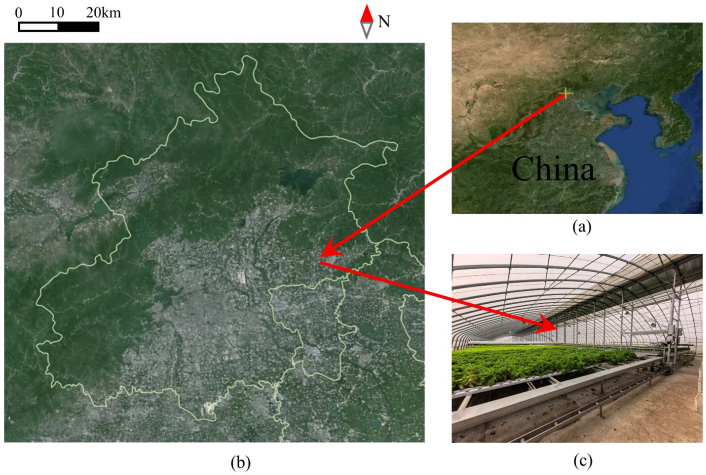


Figure 1. Study area. (**a**) Geographic location of Beijing within China; (**b**) location of study area in Beijing; (**c**) interior view of the greenhouse.

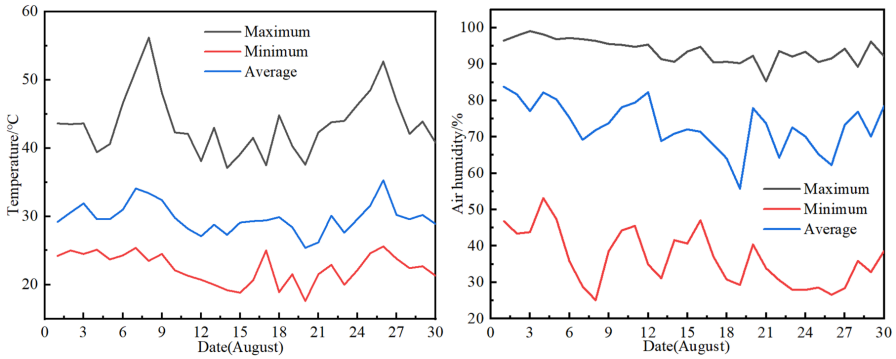


Figure 2. Daily variations in air temperature and humidity inside the greenhouse in August.

2.2. Overall Design and Working Method of the System

Building upon the existing NFT hydroponic system within the greenhouse, a nutrient solution temperature control system (NSTCS) was integrated (Figure 3). The NSTCS primarily consists of an air-source heat pump unit, a circulation pump, an integrated control cabinet, polyethylene (PE) piping, and a storage tank. The circulation pump transports the nutrient solution from the storage tank to the evaporator within the air-source heat pump unit, where heat exchange occurs, thereby enabling precise temperature regulation of the nutrient solution. To enhance the overall thermal efficiency of the system and accelerate

the equilibrium rate of cooling within the nutrient solution flow field in the storage tank, a stirring device was installed inside the tank. The cooled nutrient solution is then delivered to the root zones of the crops through the circulation system. This configuration effectively reduces the root-zone temperature of hydroponically cultivated lettuce, mitigating heat stress and enabling normal crop growth during high-temperature summer conditions.

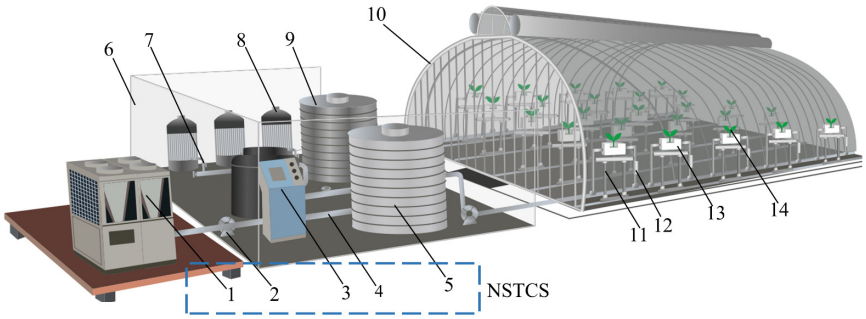


Figure 3. NSTCS layout diagram in the greenhouse. 1. Air-source heat pump unit. 2. Circulation pump. 3. Integrated control cabinet. 4. PE piping. 5. Storage tank. 6. Storage room. 7. Solenoid valve. 8. Fertilizer tank. 9. Return tank. 10. External insulation plastic greenhouse. 11. Cultivation rack. 12. Disinfection filter. 13. Cultivation trough. 14. Lettuce plants.

Figure 4 illustrates the operational principles of the NSTCS. The air-source heat pump, serving as an efficient temperature control device, operates based on the reverse Carnot cycle principle [33]. At its core, the compressor plays a pivotal role by compressing low-pressure, low-temperature refrigerant vapor into high-pressure, high-temperature vapor. This vapor then releases heat to the surrounding air as it condenses within the condenser. The electronic expansion valve regulates the flow rate and pressure drop of the refrigerant by adjusting its opening degree. The high-pressure, low-temperature liquid refrigerant undergoes throttling through the expansion valve, transforming into a low-pressure, low-temperature liquid state before entering the evaporator. Here, it absorbs significant heat from the cooling medium (the nutrient solution), thereby achieving the desired cooling effect. Additionally, the design of the four-way valve enables the reversibility of the refrigerant cycle. By reversing the flow within the heat pump unit, high-pressure gaseous refrigerant condenses and releases heat in the evaporator, generating warmth to heat the nutrient solution during winter. This functionality extends the cultivation period of crops by maintaining optimal growing conditions year-round.

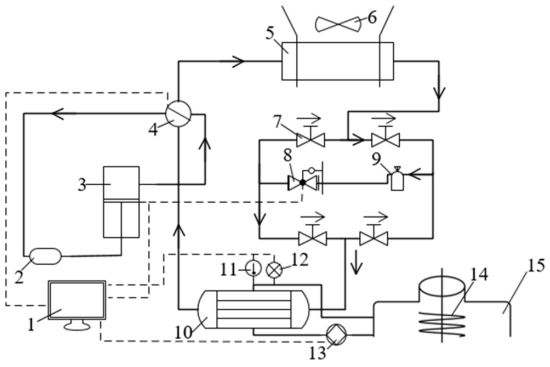


Figure 4. Schematic diagram of NSTCS. 1. controller. 2. Gas–liquid separator. 3. Compressor. 4. Four-way valve. 5. Condenser. 6. Air cooler. 7. Check valve. 8. Electronic expansion valve. 9. Refrigerant storage tank. 10. Evaporator. 11. Temperature sensor. 12. Pressure sensor. 13. Circulation pump. 14. Stirrer. 15. Storage tank.

2.3. Hardware Design of Temperature Control System

The temperature control system comprises five primary functional modules (Figure 5). The main control module performs data fusion, processing, and real-time monitoring while outputting control strategies to regulate end-effectors. The temperature acquisition module handles analog signal inputs for environmental temperature, evaporator-side temperature, nutrient solution temperature, and root-zone temperature, converting these signals into digital format. Utilizing 4G transmission technology, the data communication module enables real-time uploading of nutrient solution temperature and related parameters to the cloud platform. The output control module transmits control signals through controller ports to relays, regulating solenoid valve operations and subsequently controlling the heat pump unit, circulation pumps, and agitators via thermal relays and AC contactors. The human–machine interface and display module facilitate target temperature setting, operational mode switching, and system data exportation while providing real-time visualization of environmental conditions, nutrient solution temperature, and equipment status. The name, specification and description of the system hardware product are shown in Table 1.

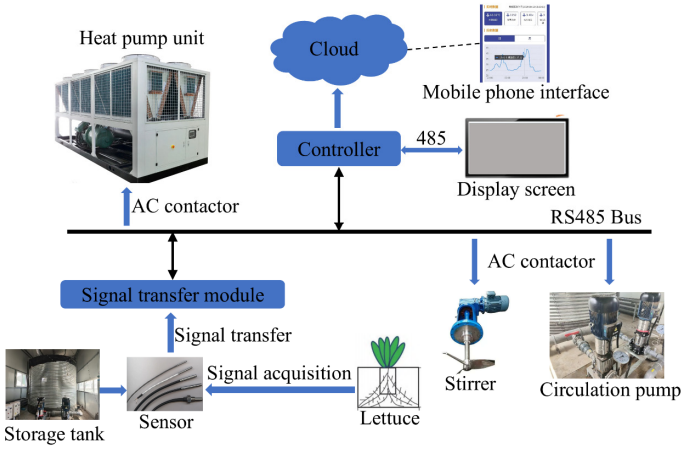


Figure 5. Design of hardware module of control system.

Table 1. Name, specification and description of system hardware product.

Product Name	Specification or Model	Product Description
Single Chip Microcomputer	STM32F103RCT6	Based on the ARM 32-bit Cortex-M architecture.
Resistive Temperature Sensor	PT100	Measurement range: −50~150 °C. Accuracy: ± 0.1 °C.
Signal Transfer Module	MAX6675	Convert analog signals into digital signals.
4G Module	Air724UG	Provide fast and reliable wireless connectivity.
AC Contactor	LC1N50	High-voltage power controller.
Thermal Relay	LRN357N	Overload protection.
Heat Pump Unit	BLD-60AH	Input power: 49.8 kW. Refrigerant: R410 A.
Solution Agitator	BLD10-1.5	Impeller diameter: 400 mm.
Circulation Pump	25CDL2-200	Input power: 2.2 kW. Lift: 150 m.

The picture of the interior of the control cabinet is shown in Figure 6. During application, certain components may be added or modified based on the actual application environment and requirements.

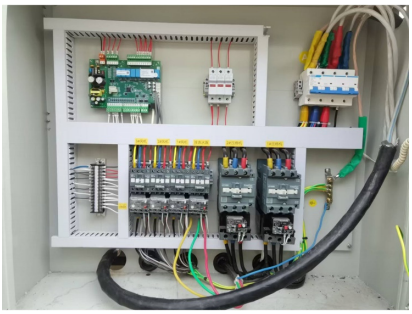


Figure 6. The interior of the control cabinet.

2.4. Control System Main Program

The temperature control system operates through the following workflow: Operators initially set nutrient solution temperature parameters via the human–machine interface. Upon system activation, power-on initialization is performed, activating the temperature detection module and enabling selection among three operational modes: automatic, cooling, and heating. In automatic mode, the system autonomously determines the operational mode based on ambient temperature readings. The main control module receives temperature signals from the detection module at specified intervals, calculating both temperature error and error rate relative to the user-defined target value. These parameters are processed through the DBO-Fuzzy PID temperature control algorithm to generate compressor frequency modulation signals. Subsequently, the controller issues operational commands to the heat pump system, regulating its heat output through precise compressor rotational speed adjustments, establishing closed-loop control of the nutrient solution temperature. Figure 7 illustrates the complete control system workflow.

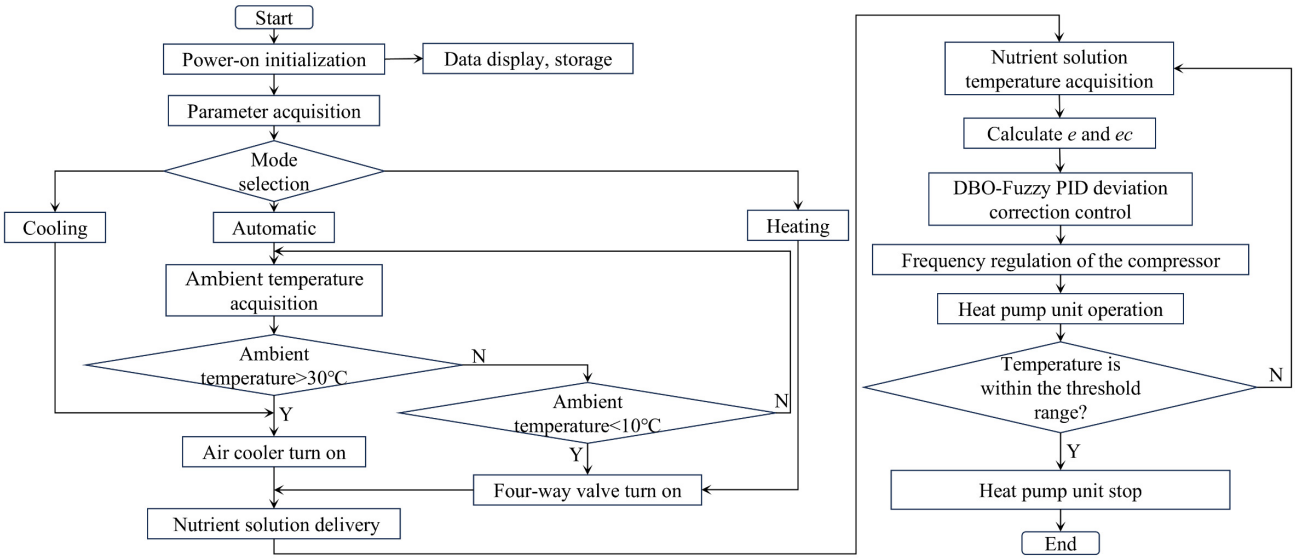


Figure 7. Workflow diagram of the control system.

2.5. Fuzzy PID Controller Design Based on Adaptive Dung Beetle Algorithm Optimization

In this study, nutrient solution temperature regulation is primarily achieved through the heat exchange components in the heat pump unit's evaporator and temperature sensor feedback. The nutrient solution undergoes mixing and agitation within the storage tank before being delivered to cultivation troughs. During this process, the nutrient solution naturally heats up due to environmental temperature influences, necessitating continuous adjustments to maintain optimal nutrient solution temperatures for lettuce growth upon reaching the cultivation troughs. To address the limitations of traditional PID control

algorithms in handling nonlinear system adaptability and precision control, an adaptive fuzzy PID controller optimized by the DBO algorithm was developed. This advanced control system dynamically adjusts to greenhouse temperature variations, ensuring precise nutrient solution temperature regulation throughout the cultivation process.

2.5.1. Mathematical Model

The transient temperature variations in nutrient solution in the storage tank are typically simulated using a single-capacity thermal model, where the liquid temperature is determined by solving a first-order ordinary differential equation. This modeling approach has been widely adopted by numerous researchers for temperature control of single-capacity fluid systems [22,34]. In this study, the energy balance process of the nutrient solution within the tank is illustrated in Figure 8, with the following simplifying assumptions: 1. The short distance between the heat pump and storage tank, combined with insulated piping, allows for negligible heat loss during solution transport; 2. The nutrient solution maintains uniform temperature distribution throughout the entire tank volume.

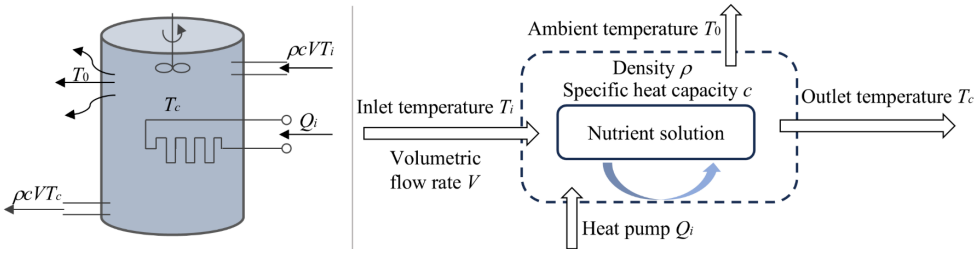


Figure 8. Energy balance diagram of nutrient solution.

Equation (1) describes the energy balance of a single-container thermal process, taking into account heat input, heat loss, and temperature dynamics of the fluid within the container. Each term in the equation has the following physical meaning: Q_i represents the heat energy added to the tank by the heat pump. For the cooling process, Q_i is negative, indicating heat removal; ρcVT_i represents the heat carried by the incoming fluid; ρcVT_c represents the heat carried away by the outgoing fluid; $hA(T_c - T_0)$ represents the heat transfer between the container and the surrounding environment via conduction, convection, or radiation; and $C \times (dT_c/dt)$ represents the rate of change in the internal fluid temperature over time, scaled by the nutrient solution's thermal capacitance C in the storage tank.

$$Q_i + \rho cVT_i - \rho cVT_c - hA(T_c - T_0) = C\frac{dT_c}{dt}, \quad (1)$$

where Q_i represents the heat energy provided by the heat pump, W; ρ denotes the density of the nutrient solution, kg/m^3; c is the specific heat capacity of the nutrient solution, J/(kg·K); V denotes the nutrient solution volumetric flow rate, m^3/s; T_i indicates the nutrient solution temperature at the inlet, °C/K; T_c represents the nutrient solution temperature at the outlet, equivalent to the temperature within the tank, °C/K; T_0 is the ambient temperature, °C/K; h is the heat transfer coefficient between the storage tank and air, W/(m^2·K); A is the heat transfer area, m^2; and C is the thermal capacitance of the nutrient solution in the storage tank, J/K.

By transforming Equation (1) into incremental form, we obtain the following:

$$\Delta Q_i + \rho cV\Delta T_i - \rho cV\Delta T_c - hA(\Delta T_c - \Delta T_0) = C\frac{d\Delta T_c}{dt}. \quad (2)$$

Let $\underline{\rho cV} = K_0$, where K_0 represents the thermal coefficient of the nutrient solution; and let $\overline{hA} = 1/R$, where R denotes the thermal resistance. By substituting these into Equation (2), we obtain the following simplified energy balance equation:

$$C\frac{d\Delta T_c}{dt} + K_0\Delta T_c = \Delta Q_i + K_0\Delta T_i - \frac{\Delta T_c - \Delta T_0}{R}. \tag{3}$$

Applying the Laplace transform to Equation (3) and rearranging yields, we obtain the following:

$$T_c(s) = \frac{\frac{R}{RK_0+1}}{\frac{R}{RK_0+1}+Cs+1}Q_i(s) + \frac{\frac{RK_0}{RK_0+1}}{\frac{R}{RK_0+1}Cs+1}T_i(s) + \frac{\frac{1}{RK_0+1}}{\frac{R}{RK_0+1}Cs+1}T_0(s). \tag{4}$$

Equation (4) represents the input/output model of the nutrient solution temperature. Assuming adiabatic conditions for the storage tank and constant return solution temperature T_i, treating ambient temperature and return solution temperature as disturbance variables, the relationship between the nutrient solution temperature T_c and the heat energy Q_i can be described by the following transfer function:

$$G(s) = \frac{\Delta T_c(s)}{\Delta Q_i(s)} = \frac{K}{Ts+1}, \tag{5}$$

where $K = R/RK_0 + 1$ represents the system gain; and $T = RC/RK_0 + 1$ denotes the system time constant. Considering the time delay τ in the heat exchange process and introducing a lag component into the transfer function, the final approximate transfer function $G(s)$ for temperature control is obtained as follows:

$$G(s) = \frac{\Delta T_c(s)}{\Delta Q_i(s)} = \frac{K}{Ts+1}e^{-\tau s}. \tag{6}$$

To ensure the accuracy of subsequent simulation results, the step response method was employed for model parameter identification. First, to minimize interference, the storage tank was insulated and the cultivation-side circulation pump was deactivated. The controller output was adjusted to produce a step change. Nutrient solution temperature within the tank was recorded every 60 s, obtaining complete input-output data approximating open-loop step response. The collected temperature data were imported into Origin 2022 for scatter plot fitting ($R^2 = 0.991$), yielding the open-loop step response curve shown in Figure 9. Using the two-point method [35], the model parameters were identified as $K = 1.7$, $T = 340$, and $\tau = 10$.

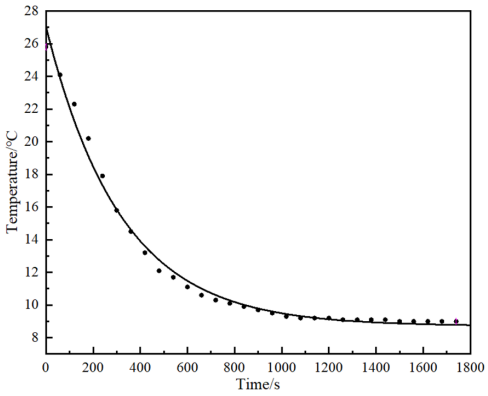


Figure 9. Open-loop step response curve of the temperature control system.

2.5.2. Fuzzy PID Controller

The PID control achieves precise regulation by generating a control signal through weighted synthesis of three components: proportional, integral, and derivative terms derived from deviation. The explicit expression for PID controller output is as follows:

$$u(t) = K_p e(t) + K_i \int_0^t e(t)dt + K_d \frac{de(t)}{dt}, \tag{7}$$

where $u(t)$ is the output of the PID controller; $e(t)$ is the deviation; and K_p, K_i, and K_d are the proportional, integral, and differential parameters of PID, respectively.

The fuzzy PID controller processes deviation signals through fuzzy logic, dynamically adjusting PID parameters (proportional coefficient K_p, integral coefficient K_i, and derivative coefficient K_d) based on temperature deviation and its rate of change. This adaptive mechanism enables the control system to effectively accommodate varying operational conditions, achieving precise regulation of the controlled variable (nutrient solution temperature). This study employs a dual-input triple-output fuzzy control architecture, comprising two main components: the fuzzy controller and the PID controller, as illustrated in Figure 10.

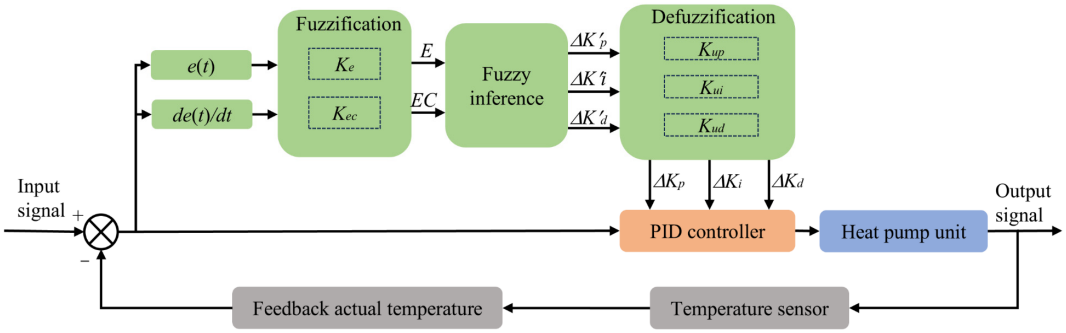


Figure 10. Schematic diagram of fuzzy PID temperature controller.

The nutrient solution temperature deviation e and its rate of change ec are selected as input variables. These inputs undergo quantization and fuzzification processes, yielding corresponding fuzzy sets E and EC. Through fuzzy rule-based inference, the fuzzy values of control parameters are determined. Subsequently, the high-precision centroid method is employed for defuzzification of the PID parameters obtained from fuzzy reasoning. Finally, the self-tuning parameters of the fuzzy PID controller (ΔK_p, ΔK_i, ΔK_d) are adjusted based on scaling factors, enabling real-time PID parameter correction. The parameter adjustment formulas for the control algorithm are as follows:

$$\begin{cases} K_p = K_{p0} + \Delta K_p \\ K_i = K_{i0} + \Delta K_i \\ K_d = K_{d0} + \Delta K_d \end{cases}, \tag{8}$$

where K_{p0}, K_{i0}, and K_{d0} are the initial values of the PID parameters.

The parameter settings of the fuzzy controller are detailed in Table 2. In practical implementation, a combination of triangular and Gaussian membership functions is selected for the temperature deviation e and its rate of change ec, while triangular membership functions are adopted for the system self-tuning output variables (ΔK_p, ΔK_i, ΔK_d). The structure of these membership functions is illustrated in Figure 11.

Prior to fuzzy inference, the actual domain values are transformed into the fuzzy domain of subsets through multiplication with quantization factors. Following defuzzification, the output parameters are adjusted using scaling factors to obtain actual control values. Based on conventional empirical formulas [36], the initial fuzzy PID parameters

before algorithm optimization are set as quantization factors K_e = 2, K_{ec} = 0.5, and scaling factors K_{up} = 0.05, K_{ui} =0.01, and K_{ud} = 0.005.

Table 2. Parameterization of fuzzy PID.

Input/Output Variables	*e*	*ec*	ΔK_p	ΔK_i	ΔK_d
Fuzzy language	*E*	*EC*	ΔK_P	ΔK_I	ΔK_D
Basic domain	[−12, 12]	[−3, 3]	[−0.3, 0.3]	[−0.06, 0.06]	[−0.03, 0.03]
Fuzzy domain	[−6, 6]	[−6, 6]	[−6, 6]	[−6, 6]	[−6, 6]
Fuzzy subset	{Positive Big (PB), Positive Middle (PM), Positive Small (PS), Zero (Z), Negative Small (NS), Negative Middle (NM), Negative Big (NB)}				

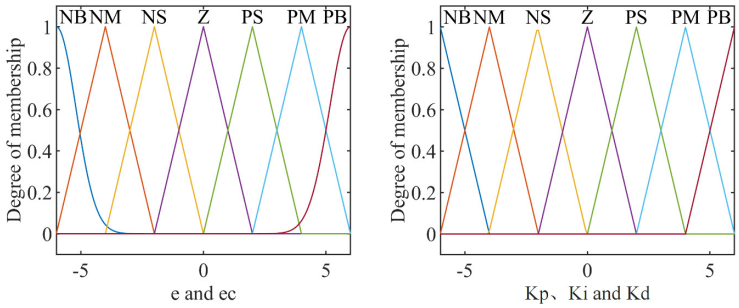


Figure 11. Membership function of the fuzzy PID controller.

The fuzzy rule base comprises a series of conditional statements following the "if *E* and *EC* then *U*" structure. The rational design of fuzzy rules is crucial for optimizing controller performance. During the initial system startup phase, when system deviation is substantial, control outputs should prioritize rapid deviation elimination and enhanced response speed. As the system approaches the target nutrient solution temperature, control outputs should emphasize system stability and minimize overshoot. Drawing upon technical knowledge and practical experience from PID tuning processes, a total of 49 fuzzy rules were designed for the controller, as detailed in Table 3.

Table 3. Table of K_p, K_i, and K_d fuzzy control rules.

E	*EC*						
	NB	**NM**	**NS**	**Z**	**PS**	**PM**	**PB**
NB	Z/NB/NS	Z/NB/NS	Z/NM/NS	Z/NS/NS	PS/PS/NS	PS/NM/PS	PS/Z/PS
NM	Z/NB/NS	Z/NB/NS	Z/NM/NS	Z/NS/NS	PS/NS/NS	PS/Z/PS	PS/Z/PM
NS	PS/NB/NS	PS/NM/NS	PS/Z/NS	PS/Z/Z	PS/Z/Z	PM/PS/PS	PM/Z/PM
Z	PS/NM/NS	PS/NM/NS	PS/NS/NS	PS/Z/Z	PS/PS/Z	PM/PM/PS	PM/PM/PM
PS	PM/Z/NS	PM/NS/NS	PM/Z/Z	PM/PS/Z	PM/PS/Z	PB/PM/PS	PB/PB/PM
PM	PM/Z/NS	PM/Z/NS	PM/PS/Z	PM/PM/PS	PM/PM/PS	PB/PB/PS	PB/PB/PB
PB	PM/Z/NS	PM/Z/NS	PM/PS/Z	PM/PM/PS	PM/PM/PS	PB/PB/PS	PB/PB/PM

2.5.3. Optimization of Fuzzy PID Based on Adaptive Dung Beetle Algorithm

The DBO algorithm simulates the social behaviors of dung beetle populations, including ball rolling, dancing, reproduction, foraging, and stealing, to achieve both local and global optimization. The population is categorized into four groups: ball-rolling dung beetles, breeding dung beetles, foraging dung beetles, and stealing dung beetles [37]. This algorithm exhibits superior solution accuracy, rapid convergence, and strong stability [38]. By integrating the DBO algorithm with the fuzzy controller, we enhance the system's effectiveness through optimal selection of quantization and scaling factors, along with

adaptive weight adjustment. This integration enables improved control performance. The position update rules for each dung beetle group are as follows.

In the absence of obstacles, ball-rolling dung beetles maintain linear movement of dung balls by utilizing celestial cues. The position update is described as follows:

$$x_i(t+1) = x_i(t) + amx_i(t-1) + b|x_i(t) - x_{worst}(t)|, \tag{9}$$

where $x_i(t)$ represents the position of the i-th dung beetle at the t-th iteration; a denotes the natural factor causing deviation from the original direction; $m \in (0, 0.2]$ and $b \in (0, 1]$ are random numbers; $x_{worst}(t)$ indicates the global worst position; and $|x_i(t) - x_{worst}(t)|$ simulates light intensity variation, where higher values correspond to weaker light sources.

When encountering obstacles, dung beetles adjust their direction through dancing behavior, which is simulated using the tangent function. The position update is formulated as follows:

$$x_i(t+1) = x_i(t) + \tan\theta|x_i(t) - x_i(t-1)|, \tag{10}$$

where $\theta \in [0, \pi]$ represents the deviation angle; when $\theta = 0$ or $\pi/2$, the dung beetle maintains its position; and $|x_i(t) - x_i(t-1)|$ denotes the positional offset of the i-th dung beetle between the t-th and $(t-1)$-th iterations.

The oviposition area of female breeding dung beetles is simulated using a boundary selection strategy. The position update is formulated as follows:

$$x_i(t+1) = x_{gbest}(t) + b_1[x_i(t) - L_{b*}] + b_2[x_i(t) - U_{b*}], \tag{11}$$

where $x_{gbest}(t)$ represents the global best position; b_1 and b_2 are two independent random vectors of size $1 \times d$, where d denotes the dimensionality of the optimization problem; and L_{b^*} and U_{b^*} indicate the lower and upper bounds of the breeding region, respectively.

Breeding dung beetles deposit eggs within dung balls, which develop into foraging dung beetles. These foraging individuals navigate toward the optimal foraging area, with their position update during foraging described as follows:

$$x_i(t+1) = x_i(t) + C_1[x_i(t) - L_{bl}] + C_2|x_i(t) - U_{bl}|, \tag{12}$$

where L_{bl} and U_{bl} represent the lower and upper bounds of the foraging area, respectively; C_1 is a random number following normal distribution; and C_2 is a random vector of size $1 \times$ d.

During foraging, some stealing dung beetles pilfer dung balls from others within the foraging area. The position update during thieving behavior is formulated as follows:

$$x_i(t+1) = x_{lbest}(t) + Qg(\left|x_i(t) - x_{gbest}(t)\right| + |x_i(t) - x_{lbest}(t)|), \tag{13}$$

where $x_{lbest}(t)$ represents the optimal food source at iteration t; Q denotes a constant value; and g is a $1 \times$ d random vector following normal distribution.

The DBO algorithm is employed to optimize the fuzzy PID parameters, including quantization factors (K_e, K_{ec}) and scaling factors (K_{up}, K_{ui}, K_{ud}). Through iterative population optimization, the fitness function is computed to identify optimal parameters, thereby enhancing system stability and robustness while overcoming the limitations of manual tuning. The process begins with setting the algorithm parameters and initializing the dung beetle population, which consists of 40 individuals distributed in a ratio of 4:4:5:7, with a maximum of 20 iterations. Next, the fitness value of each individual is evaluated using Equation (14) as the fitness function, where a lower *ITAE* value signifies that the system's response is closer to the ideal state. The positions of the dung beetles are updated

according to Equations (9)–(13), and the fitness values of all individuals are compared with the current minimum fitness value to update both the minimum value and the optimal position. Finally, if the maximum number of iterations is reached, the algorithm outputs the optimal dung beetle position parameters, representing the best quantization and scaling factors. The entire optimization process is illustrated in Figure 12.

$$ITAE = \int_0^t t|e(t)|dt \tag{14}$$

where t represents the system operating time; and $|e(t)|$ denotes the absolute error between the setpoint and actual values of the nutrient solution temperature.

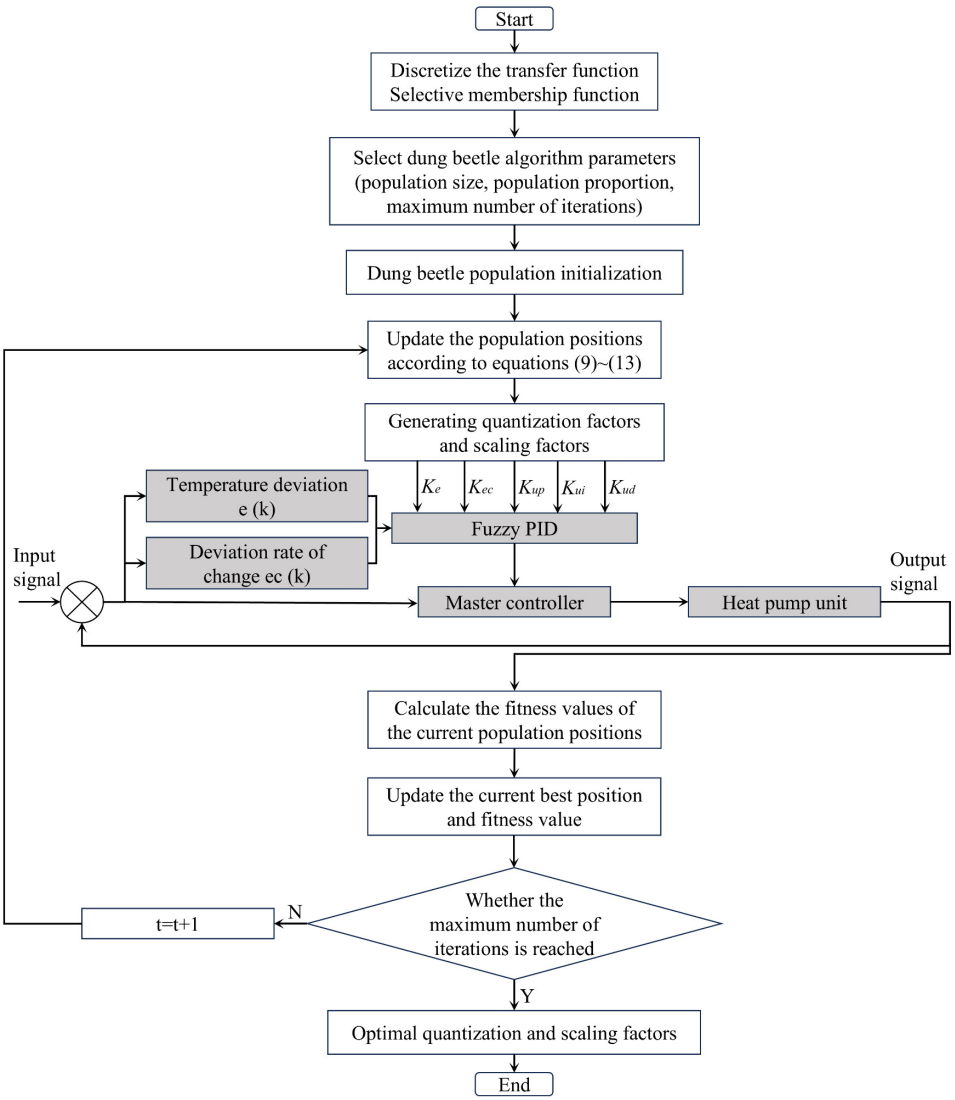


Figure 12. Flowchart of adaptive dung beetle algorithm for optimizing quantization and scaling factors.

The iterative optimization process of the adaptive DBO algorithm is illustrated in Figure 13. The algorithm achieves convergence after 10 iterations, with the optimal solution yielding a fitness value of 297.63. Through position analysis, the optimized fuzzy PID parameters are determined as quantization factors K_e = 0.159 and K_{ec} = 0.915, along with scaling factors K_{up} = 1.502, K_{ui} = 0.018, and K_{ud} = 0.021. Utilizing MATLAB 2024a's fuzzy PID design toolbox, the relevant parameters were configured, resulting in a fuzzy PID controller optimized by the adaptive DBO algorithm.

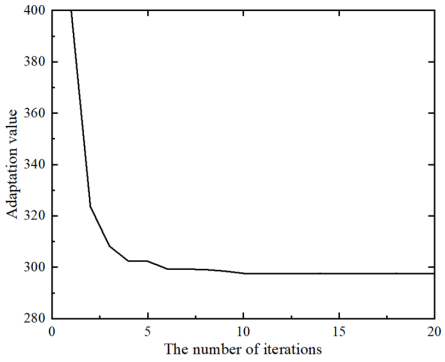


Figure 13. Iterative optimization of dung beetle algorithm.

3. Experiments and Results

3.1. Simulation Experiment

To validate the effectiveness of the DBO-Fuzzy PID temperature control algorithm, a simulation model of the DBO-optimized Fuzzy PID controller was developed using the Simulink toolbox in MATLAB 2024a, as illustrated in Figure 14. A step signal was employed as the system's desired input to compare the step response curves of three control algorithms: conventional PID, fuzzy PID, and DBO-Fuzzy PID. An interference signal was introduced during the simulation to evaluate the anti-disturbance performance of each control method. The step change represents one of the most stringent forms of disturbance in control systems and is also the most convenient for computation and implementation. As the most representative signal, satisfactory control performance under step disturbance typically indicates effective handling of other disturbance types.

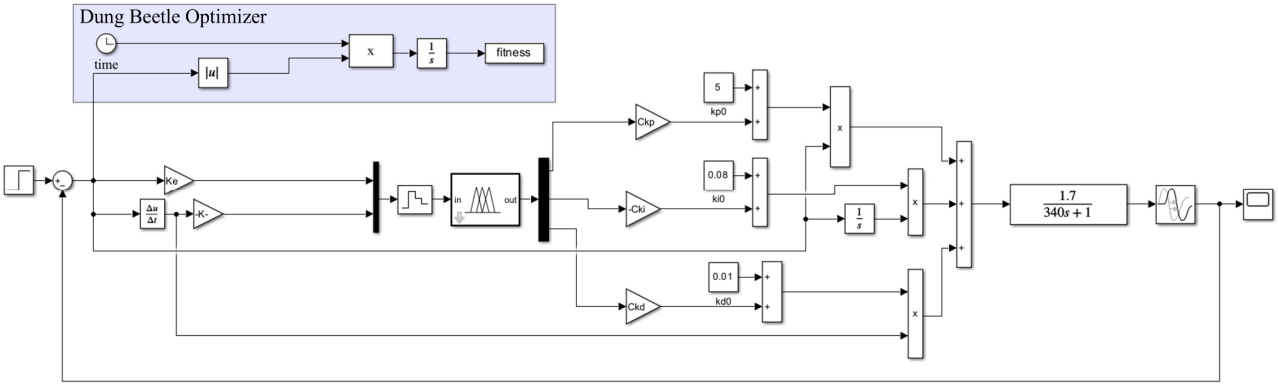


Figure 14. Simulink model of DBO-Fuzzy PID controller.

We evaluated the dynamic and steady-state performance of the three control methods using three key metrics: settling time, overshoot, and steady-state error. In control theory, settling time is defined as the shortest time required for the controlled variable to enter and remain within ±5% of the new steady-state value. Overshoot refers to the ratio of the maximum instantaneous deviation to the steady-state value of the controlled variable. Steady-state error represents the deviation that occurs when the system transitions from one steady state to another.

The step response curves of DBO-Fuzzy PID, conventional PID, and fuzzy PID controllers were compared, with results shown in Figure 15 and Table 4. The DBO-Fuzzy PID controller demonstrated superior performance among the three methods, achieving a settling time of 35.23 s, which represents reductions of 165.13 s and 123.19 s compared to PID and fuzzy PID, respectively. The overshoot was 2.18%, lower than PID and fuzzy PID by 22.32% and 6.92%, respectively. The steady-state error reached a minimum of

0.009 °C. These results indicate that the DBO-Fuzzy PID control method provides faster and smoother responses to step signals with improved regulation accuracy.

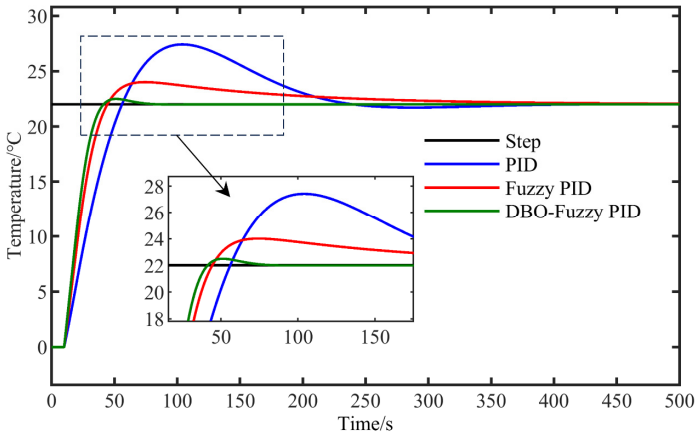


Figure 15. Comparison of step response curves of three control methods without disturbance.

Table 4. Evaluation indicators.

Control Method	Settling Time/s	Overshoot/%	Steady-State Error/°C
PID	200.36	24.50	0.035
Fuzzy PID	158.42	9.10	0.016
DBO-Fuzzy PID	35.23	2.18	0.009

The simulation results under disturbance signals are shown in Figure 16. When subjected to external disturbances such as changes in nutrient solution volume or ambient temperature, causing deviations from the target temperature, the DBO-Fuzzy PID controller demonstrates faster and more stable disturbance rejection, achieving rapid stabilization. Unlike fuzzy PID control, where quantization and scaling factors are manually adjusted, the DBO-Fuzzy PID controller optimizes these parameters through iterative dung beetle population optimization and fitness function evaluation. Consequently, the designed DBO-Fuzzy PID controller meets the requirements for nutrient solution temperature control, exhibiting enhanced stability and robustness.

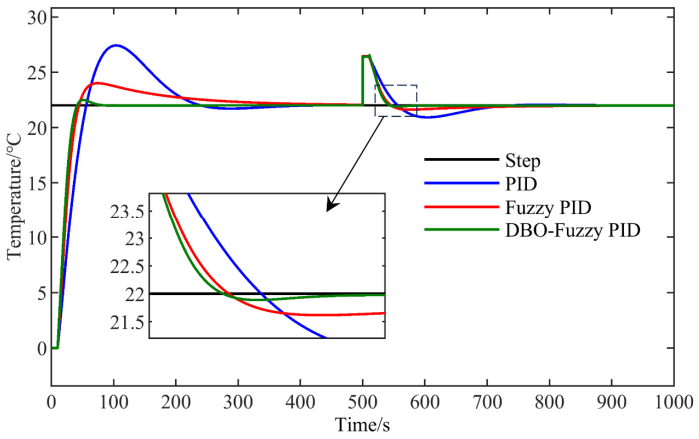


Figure 16. Comparison of step response curves of three control methods with disturbance.

3.2. Field Experients

3.2.1. Verification Test of Performance

Three equal-sized areas (A, B, and C) were established within the cultivation beds for system testing, each equipped with an independent storage tank and nutrient solution

circulation device. Area A served as the control group, with sensor nodes only deployed at the storage tank outlet to monitor nutrient solution temperature without cooling. Areas B and C were equipped with both sensor nodes and temperature control systems to enable intelligent regulation, validating the performance of traditional PID control and adaptive DBO-Fuzzy PID optimized cooling systems, respectively. According to previous studies [39], 22 °C represents the optimal nutrient solution temperature for NFT hydroponic lettuce cultivation. Figure 17 illustrates the nutrient solution temperature variations under typical summer conditions (8 August 2024).

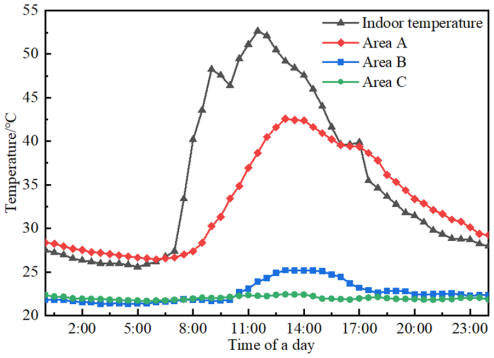


Figure 17. Graph of nutrient solution temperature.

Figure 17 demonstrates that the average nutrient solution temperatures in areas B and C were 22.60 °C and 21.98 °C, respectively, both close to the optimal temperature (22 °C) for lettuce growth, consistent with expected cooling performance. However, during the high-temperature period from 11:00 to 17:00, the deviation from the optimal temperature increased in area B, indicating that traditional PID control lacks adaptive capability under extreme environmental variations. Area A maintained an average nutrient solution temperature of 32.76 °C, significantly higher than the optimal temperature. Figure 18 illustrates the deviation between the nutrient solution temperature and the optimal temperature (22 °C) for error analysis, with the vertical axis representing the temperature difference.

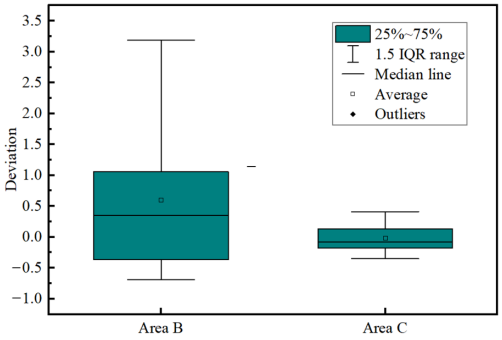


Figure 18. Box plot of the difference between nutrient solution temperature and optimal temperature.

Error analysis was conducted on the nutrient solution temperatures in areas B and C. Area C exhibited smaller average deviation and median values compared to area B. The narrower interquartile range and absence of outliers in area C's boxplot indicate that its nutrient solution temperature remained closer to the optimal value (22 °C), with a smaller variation range. Compared to traditional control methods, the smart nutrient solution temperature control system utilizing adaptive DBO-Fuzzy PID demonstrates superior performance, maintaining temperatures closer to the optimal range for lettuce growth. This system enables faster temperature adjustment, higher control precision, improved robustness, and enhanced practical applicability.

3.2.2. Verification Test of Cultivation

The experiment utilized the lettuce cultivar 'Spanish Green', with seedlings cultivated by the Vegetable Research Center of the Beijing Academy of Agriculture and Forestry Sciences. After 20 days of artificial light seedling cultivation in a climate-controlled chamber, uniformly sized seedlings were transplanted onto NFT cultivation beds in areas A, B, and C on 2 August 2024, comprising three treatments with three replicates each (36 plants per replicate). Each area's storage tank contained an initial nutrient solution volume of 300 L, circulated between the tank and cultivation troughs at a flow rate of 750 ± 20 mL/min using a continuous supply system. The nutrient solution followed a specialized formulation for hydroponic leafy vegetables, maintained at EC 2.0 ± 0.1 mS/cm and pH 6.0 ± 0.2 throughout the cultivation period. All lettuce plants were harvested on August 30, with the overall appearance of plants from each area shown in Figure 19. Fresh and dry weights of roots and leaves were measured using a precision electronic balance (JM-BL5003), with results presented in Table 5.



Figure 19. The overall appearance of plants from each area.

Table 5. Growth status of lettuce under different nutrient solution temperature treatments.

Group	Root Fresh Weight/g	Root Dry Weight/g	Leaf Fresh Weight/g	Leaf Dry Weight/g
Area A	6.48 ± 1.31c	0.27 ± 0.02c	47.26 ± 5.07b	2.11 ± 0.12c
Area B	8.61 ± 1.19b	0.32 ± 0.02b	70.87 ± 2.84a	3.05 ± 0.08b
Area C	9.48 ± 1.21a	0.36 ± 0.01a	74.01 ± 2.23a	3.23 ± 0.07a

Note: Means within each column followed by the same letters are not significantly different according to Duncan's multiple range test at $p < 0.05$.

As shown in Table 5, the fresh root weights in areas B and C increased by 24.74% and 31.65%, respectively, compared to area A. Similarly, fresh leaf weights in areas B and C showed increases of 33.31% and 36.14%, respectively, over area A. These results demonstrate that the designed nutrient solution temperature control system effectively mitigates heat stress in lettuce through root-zone cooling, promoting biomass accumulation. Furthermore, the superior biomass accumulation in area C compared to area B validates the practical effectiveness of the adaptive DBO-Fuzzy PID algorithm.

4. Discussion

Currently, research on localized cooling techniques in greenhouses to mitigate heat stress has extensively explored crop physiological characteristics and stress damage mechanisms [4,40]. A series of innovative root-zone cooling systems suitable for hydroponics or substrate-based cultivation have been developed [18,41,42], which are of significant importance in reducing costs and improving crop yields in climate-challenging regions. Previous studies have primarily emphasized the design and modification of system configurations, but the regulation methods have been relatively rudimentary. In this study, while refining the structural design of the system, emphasis was placed on precise management

of nutrient solution temperature. The NSTCS designed in this work achieved automatic temperature monitoring and operation of cooling devices. Under the control of the DBO-Fuzzy PID controller, the system demonstrated adaptive adjustment of the nutrient solution temperature. Compared to temperature control systems using conventional PID control, the proposed system exhibited more stable temperature regulation and enhanced adaptability to the high-temperature environment of greenhouses.

This study focuses on the widely applied fuzzy PID control method and combines it with the novel DBO algorithm, achieving significant results. Cao et al. optimized fuzzy PID parameters using the DBO algorithm [37], resulting in approximately a 40s reduction in stabilization time, a 7% decrease in overshoot, and the near elimination of steady-state error compared to standard fuzzy PID systems. Experimental validation demonstrated that this controller improved the overall temperature uniformity of four-bar targets and enhanced the detection accuracy of infrared thermography. Similarly, Zhang et al. integrated DBO with fuzzy PID control [43], revealing that the DBO-Fuzzy PID controller significantly reduced body acceleration under random disturbances compared to passive suspension systems. These findings collectively suggest that reasonable modifications to Fuzzy-PID algorithms can accelerate optimization of critical parameters, enhance control precision, and strengthen disturbance rejection capabilities–advantages that align closely with the results of the present study. When the nutrient solution temperature target was set at 22 °C, the system demonstrated superior cooling performance. Comparative analysis revealed 31.65% and 36.14% increases in root fresh weight and leaf fresh weight of lettuce, respectively, compared to non-cooled treatments. These results are consistent with findings from Silva et al. [9], Levine et al. [10], Thanulla et al. [11], and Li et al. [15], who reported significant improvements in root and shoot biomass accumulation in lettuce through hydroponic nutrient solution cooling during high-temperature periods. As shown in Table 5, Area C exhibited greater biomass accumulation than Area B, a discrepancy potentially attributable to dissolved oxygen decline in Area B's nutrient solution during thermal elevation episodes, coupled with lettuce's high thermal sensitivity.

On the other hand, according to the No Free Lunch (NFL) Theorem, no algorithm can be unconditionally regarded as optimal. As demonstrated by Hu et al. [44], the initial population of the DBO algorithm is randomly generated, which suppresses population diversity. Furthermore, the fixed ratio of the population fails to achieve a balance between local exploitation and global search capabilities; these limitations require further improvement. Notably, the superiority of the proposed system in this study is realized under specific conditions, including temperature control devices, agronomic practices, and single-crop and seasonal scenarios. Its applicability may be constrained by factors such as climate variations, hardware performance of the system, and crops with differing thermal sensitivities and root zone requirements. Although the research outcomes provide a theoretical foundation and practical reference for achieving accurate and stable control of hydroponic nutrient solution temperature, in real-world applications, algorithm parameters may require adjustments and optimization based on specific system configurations and layouts. In future work, we aim to enhance the system's adaptability to diverse climates and heat-sensitive crops through configuration optimization and algorithm upgrades, followed by comprehensive seasonal testing and cultivation trials to thoroughly evaluate system performance. Additionally, the initial costs and operational expenses of the system will be assessed to determine the investment payback period.

5. Conclusions

The summer cultivation of lettuce in greenhouses frequently encounters heat stress challenges. In hydroponic systems, cooling the nutrient solution to reduce root zone tem-

perature is an effective strategy to alleviate heat stress. To address the issue of temperature control instability in hydroponic nutrient solutions under high-temperature conditions, this study developed a nutrient solution temperature control system based on an adaptive DBO-fuzzy PID controller. Firstly, the system integrates high-precision sensor networks and air-source heat pump units, forming the hardware foundation of the system. Simultaneously, a fuzzy PID controller optimized by the DBO algorithm was designed for this system, enabling real-time adjustment of quantization and scaling factors in the fuzzy controller.

Comparative simulation experiments of the adaptive DBO-optimized fuzzy PID controller demonstrated superior performance: the DBO-Fuzzy PID achieved a settling time of 35.2 s, representing reductions of 165.1 s and 123.2 s compared to conventional PID and fuzzy PID controllers, respectively. The overshoot was 2.2%, lower than conventional PID and fuzzy PID by 22.3% and 6.9%, respectively. When subjected to disturbance signals, the DBO-Fuzzy PID controller exhibited faster and more stable disturbance rejection, demonstrating enhanced stability and robustness.

System performance tests in the summer greenhouse demonstrated that the DBO-Fuzzy PID optimized nutrient solution temperature control system exhibited better adaptability to high-temperature environments compared to traditional PID control. Cultivation experiments revealed that lettuce grown with traditional PID and DBO-Fuzzy PID temperature control showed fresh root weight increases of 24.7% and 31.7%, respectively, and fresh leaf weight increases of 33.3% and 36.1%, respectively, compared to non-cooled conditions. These results confirm the system's effectiveness in mitigating heat stress and maintaining optimal nutrient solution temperatures for lettuce growth. The results can provide a theoretical basis and practical reference for precise and stable temperature control in hydroponic nutrient solutions.

Author Contributions: Conceptualization, W.G., H.X., Y.T. and L.W.; methodology, W.G. and Y.C.; software, X.H. and Q.Z.; validation, Y.C., W.G. and Z.Z.; formal analysis, Y.C.; investigation, W.G. and H.X.; resources, W.G. and Q.Z.; data curation, Y.C. and Z.Z.; writing—original draft preparation, Y.C.; writing—review and editing, W.G.; visualization, Y.C.; supervision, W.G., Z.Z. and X.H.; project administration, W.G. and Z.Z.; funding acquisition, W.G. and H.X. All authors have read and agreed to the published version of the manuscript.

Funding: This research was funded by the Special Program for International Science and Technology Cooperation, Ningxia Academy of Agriculture and Forestry Sciences (DW-X-2023001) and the research and demonstration on the integration of modern technologies and equipment between China and the Netherlands in facility vegetables in Pinggu (Z221100006422008).

Institutional Review Board Statement: Not applicable.

Informed Consent Statement: Not applicable.

Data Availability Statement: The original contributions presented in the study are included in the article; further inquiries can be directed to the corresponding author.

Acknowledgments: We thank all the authors for their support. The authors are also very grateful for the kind suggestions and valuable comments by the anonymous reviewers.

Conflicts of Interest: The authors declare no conflicts of interest.

Abbreviations

The following abbreviations are used in this manuscript:

PID	Proportional–Integral–Derivative
DBO	Dung Beetle Optimizer
NSTCS	nutrient solution temperature control system
NFT	Nutrient Film Technique

References

1. Park, M.; Kang, T.; Yun, S.; Lim, R.; Son, J.; Kang, D. Analysis and monitoring of environmental parameters in a single-span greenhouse during strawberry cultivation. *J. Environ. Sci. Int.* **2021**, *30*, 907–914. [CrossRef]
2. Liu, Y.; Chen, Y.; Fu, Y.; Zeng, L.; Wang, X.; Zhu, G. Influence of Cutting Regeneration Technique at High Density on Physiological Growth of Oversummering Hydroponics Lettuce in Hainan. *China Cucurbits Veg.* **2018**, *31*, 12–16, (In Chinese with English Abstract).
3. Rahman, M.A.; Chakraborty, N.R.; Sufiun, A.; Banshal, S.K.; Tajnin, F.R. An AIoT-based Hydroponic System for Crop Recommendation and Nutrient Parameter Monitorization. *Smart Agric. Technol.* **2024**, *8*, 100472. [CrossRef]
4. Song, M.; Wen, X.; Li, Y. Effects of High Rhizosphere Temperature on Plant Growth and Metabolism: A review. *Chin. J. Ecol.* **2010**, *29*, 2258–2264, (In Chinese with English Abstract).
5. Kun, L.I.; Hui, F.; Zou, Z.R.; Cheng, R. Optimization of Rhizosphere Cooling Airflow for Microclimate Regulation and Its Effects on Lettuce Growth in Plant Factory. *J. Integr. Agric.* **2021**, *20*, 2680–2695.
6. Cortella, G.; Saro, O.; De Angelis, A. Temperature Control of Nutrient Solution in Floating System Cultivation. *Appl. Therm. Eng.* **2014**, *73*, 1055–1065. [CrossRef]
7. Hooks, T.; Sun, L.; Kong, Y.; Masabni, J.; Niu, G. Effect of Nutrient Solution Cooling in Summer and Heating in Winter on the Performance of Baby Leafy Vegetables in Deep-water Hydroponic Systems. *Horticulturae* **2022**, *8*, 749. [CrossRef]
8. Hu, J.; Yang, Y.; Li, Y.; Hou, J.; Sun, Z.; Wang, H.; He, D. Analysis and Prospect of the Environment Control Systems for Greenhouse. *Trans. CSAE* **2024**, *40*, 112–128, (In Chinese with English Abstract).
9. Silva, S.; Nascimento, R.; Oliveira, H.; Cardoso, J.A.F.; Xavier, D.A.; Silva, S.S. Levels of Nitrate, Pigments and Thermographic Analysis of Lettuce under Different Temperatures of Nutrient Solution. *Afr. J. Agric. Res.* **2016**, *11*, 1668–1673.
10. Levine, C.P.; Hayashi, S.; Ohmori, Y.; Kusano, M.; Kobayashi, M.; Nishizawa, T. Controlling Root Zone Temperature Improves Plant Growth and Pigments in Hydroponic Lettuce. *Ann. Bot.* **2023**, *132*, 455–470. [CrossRef]
11. Thanulla, D.; Dunn, B.; Hu, B.; Goad, C.; Maness, N. Nutrient Solution Temperature Affects Growth and Brix Parameters of Seventeen Lettuce Cultivars Grown in an NFT Hydroponic System. *Horticulturae* **2021**, *7*, 321. [CrossRef]
12. Fussy, A.; Papenbrock, J. An Overview of Soil and Soilless Cultivation Techniques—Chances, Challenges and the Neglected Question of Sustainability. *Plants* **2022**, *11*, 1153. [CrossRef] [PubMed]
13. Lee, J.S.; Chandra, D.; Son, J. Growth, Physicochemical, Nutritional, and Postharvest Qualities of Leaf Lettuce (*Lactuca sativa* L.) as Affected by Cultivar and Amount of Applied Nutrient Solution. *Horticulturae* **2022**, *8*, 436. [CrossRef]
14. Majid, M.; Khan, J.N.; Shah, Q.M.A.; Masoodi, K.Z.; Afroza, B.; Parvaze, S. Evaluation of Hydroponic Systems for the Cultivation of Lettuce (*Lactuca sativa* L., var. Longifolia) and Comparison with Protected Soil-based Cultivation. *Agric. Water Manag.* **2021**, *245*, 106572. [CrossRef]
15. Li, F.; Chen, X. Response of Over-summer Hydroponic Lettuce to Nutrient Solution Temperature Control. *Agric. Sci. Technol.* **2017**, *18*, 1072.
16. Falah, M.A.F.; Wajima, T.; Yasutake, D. Responses of Root Uptake to High Temperature of Tomato Plants (*Lycopersicon esculentum* Mill.) in Soil-less culture. *J. Agric. Technol.* **2010**, *6*, 543–558.
17. Al-Rawahy, M.S.; Al-Rawahy, S.A.; Al-Mulla, Y.A.; Nadaf, S.K. Influence of nutrient solution temperature on its oxygen level and growth, yield and quality of hydroponic cucumber. *J. Agric. Sci.* **2019**, *11*, 75–92. [CrossRef]
18. Myung, J.; Cui, M.; Lee, B.; Lee, H.; Shin, J.; Chun, C. Development of A Root-zone Temperature Control System using Air-source Heat Pump and its Impact on the Growth and Yield of Paprika. *AoB Plants* **2024**, *16*, plae047. [CrossRef]
19. Zhou, J.; Bu, C.; Huang, D.; Niu, Q. Application and Analysis of Soilless Culture System with Adjustable Rhizosphere Temperature in Winter Tomato Production. *China Veg.* **2020**, *8*, 41–47, (In Chinese with English Abstract).
20. Walker, J.M. One-degree increments in soil temperatures affect maize seedling behavior. *Soil Sci. Soc. Am. J.* **1969**, *33*, 729–736. [CrossRef]
21. Wang, J.F.; Xu, H.; Wang, K.; Xie, J.; Yu, K.S.; Ye, G.S.; Jiang, J.L.; Han, X.R. Performance Analysis and PID Control Strategy Optimization of the Electronic Expansion Valve on the Single-tube Heat Exchange Experimental Platform. *Appl. Therm. Eng.* **2024**, *250*, 123532. [CrossRef]
22. Taler, D.; Sobota, T.; Jaremkiewicz, M.; Taler, J. Control of the temperature in the hot liquid tank by using a digital PID controller considering the random errors of the thermometer indications. *Energy* **2022**, *239*, 122771. [CrossRef]
23. He, G.; Cai, X.; Bai, Y.; Zhu, L.; Wang, D.; Hou, Y. Design and Test of Temperature Control System of Calf Milk Replacer Solution based on Fuzzy PID. *Trans. Chin. Soc. Agric. Mach.* **2022**, *53*, 266–276, (In Chinese with English Abstract).
24. Sheng, T.; Luo, H.; Wu, M. Design and Simulation of a Multi-channel Biomass Hot Air Furnace with an Intelligent Temperature Control System. *Agriculture* **2024**, *14*, 419. [CrossRef]
25. Tang, H.; Ma, R.; Chen, Y.; Huang, L.; Jiao, R. Temperature Regulation of Hot Vapor Preservation Treatment of Litchi Based on PSO-Fuzzy PID. *Appl. Sci.* **2023**, *13*, 6888. [CrossRef]

26. Meng, J.; Gao, H.; Ruan, M.; Guo, H.; Zhou, X.; Zhang, D. Design of vacuum annealing furnace temperature control system based on GA-Fuzzy-PID algorithm. *PLoS ONE* **2023**, *18*, e0293823. [CrossRef] [PubMed]
27. Qin, Z.; Wang, X.; Zhang, H.; Liu, F.; Yin, C.; Han, Z.; Weng, W. Research on heat pump air conditioner compressor speed control strategy based on whale algorithm. *Case Stud. Therm. Eng.* **2024**, *53*, 103939. [CrossRef]
28. Xue, J.; Shen, B. Dung Beetle Optimizer: A New Meta-heuristic Algorithm for Global Optimization. *J. Supercomput.* **2023**, *79*, 7305–7336. [CrossRef]
29. Zhou, Y.; He, Y.; Xing, Z.; Shao, K.; Li, Z.; Lei, L. Power Transformer Vibration Signal Prediction based on IDBO-ARIMA. *J. Electron. Meas. Instrum.* **2023**, *37*, 11–20, (In Chinese with English Abstract).
30. Rehman, S.; Menesy, A.S.; Zayed, M.E.; Zaery, M.; Al-Shaikhi, A. Synergistic sizing and energy management strategy of combined offshore wind with solar floating PV system for green hydrogen and electricity co-production using multi-objective dung beetle optimization. *Results Eng.* **2025**, *25*, 104399. [CrossRef]
31. Long, Z.; Li, J.; Yang, H.; Chen, W.; Zhang, G.; Wang, B.; Wang, W. Methods and experiments for automatic control of surface back pressure based on dung beetle optimizer-PID controller. *Process Saf. Environ. Prot.* **2024**, *191*, 360–374. [CrossRef]
32. Zhong, K.; Li, Y.; Huan, W.; Weng, X.; Wu, B.; Chen, Z.; Liang, H.; Feng, H. A novel near infrared spectroscopy analytical strategy for soil nutrients detection based on the DBO-SVR method. *Spectrochim. Acta Part A Mol. Biomol. Spectrosc.* **2024**, *315*, 124259. [CrossRef]
33. Wu, Z.; Sha, L.; Zhao, M.; Wang, X.; Ma, H.; Zhang, Y. Performance Analyses and Optimization of a Reverse Carnot Cycle-organic Rankine Cycle Dual-function System. *Energy Convers. Manag.* **2020**, *212*, 112787. [CrossRef]
34. Lakshmanan, V.; Sæle, H.; Degefa, M.Z. Electric water heater flexibility potential and activation impact in system operator perspective–Norwegian scenario case study. *Energy* **2021**, *236*, 121490. [CrossRef]
35. Yang, Y.; Pan, Y.; Zhao, Y. *Process Control and Automatic Instruments*, 3rd ed.; China Machine Press: Beijing, China, 2017; pp. 125–132.
36. Xie, J.; Chen, Y.; Gao, P.; Sun, D.; Xue, X.; Yin, D.; Han, Y.; Wang, W. Smart Fuzzy Irrigation System for Litchi Orchards. *Comput. Electron. Agric.* **2022**, *201*, 107287. [CrossRef]
37. Cao, W.; Liu, Z.; Song, H.; Li, G.; Quan, B. Dung Beetle Optimized Fuzzy PID Algorithm Applied in Four-Bar Target Temperature Control System. *Appl. Sci.* **2024**, *14*, 4168. [CrossRef]
38. Liu, Y.; Ding, X.; Wang, H.; Li, K.; Zhang, G.; Yi, Y.; Pan, S. Prediction Model for Winter and Summer Lettuce Root Zone Temperature based on Dung Beetle Algorithm to Optimize BP. *Trans. Chin. Soc. Agric. Eng.* **2024**, *40*, 231–238, (In Chinese with English Abstract).
39. Cui, J. Plant Growth, Quality and Elemental Absorption of Lettuce as Affected by Nutrient Solution Heating in Intermittent Fluid Supply Nutrient Film Technique System. *Mol. Plant Breed.* **2024**, *10*, 1–10, (In Chinese with English Abstract).
40. Li, H.; Lu, M.; Yuan, K.; Zhang, M.; Wang, D.; Hu, J. Acquisition and analysis of the optimal nutrient solution temperature range for lettuce using U-chord curvature. *Int. J. Agric. Biol. Eng.* **2024**, *17*, 93–100. [CrossRef]
41. Nisar, M.M.; Mahmood, R.; Tayyab, S.; Anees, M.; Nadeem, F. Comparative efficacy of non-electric cooling techniques to reduce nutrient solution temperature for the sustainable cultivation of summer vegetables in open-air hydroponics. *Front. Plant Sci.* **2024**, *15*, 1340641.
42. Zhang, Y.; Ni, X.; Zhang, K.; Xu, Y. Cooling performance for temato root zone with intelligence ecological planting matrix temperature control system driven by photovoltaic in greenhouse. *Trans. Chin. Soc. Agric. Eng.* **2020**, *36*, 212–219, (In Chinese with English Abstract).
43. Zhang, K.; As'arry, A.; Zhu, L.; Hairuddin, A.A.; Hassan, M.K.; Zain, M.Z.M. Enhancing ride comfort of semi-active suspension through collaboration control using dung beetle optimizer optimized Fuzzy PID controller. *Adv. Mech. Eng.* **2025**, *17*, 16878132251314332. [CrossRef]
44. Hu, C.; Wu, F.; Zou, H. New PID parameter tuning based on improved dung beetle optimization algorithm. *Can. J. Chem. Eng.* **2024**, *102*, 4297–4316. [CrossRef]

Disclaimer/Publisher's Note: The statements, opinions and data contained in all publications are solely those of the individual author(s) and contributor(s) and not of MDPI and/or the editor(s). MDPI and/or the editor(s) disclaim responsibility for any injury to people or property resulting from any ideas, methods, instructions or products referred to in the content.